

Search for a pentaquark state decaying into pJ/ψ in $\Upsilon(1, 2S)$ inclusive decays at Belle

X. Dong , H. Y. Zhang , X. L. Wang , I. Adachi , J. K. Ahn , H. Aihara ,
S. Al Said , D. M. Asner , H. Atmacan , R. Ayad , S. Bahinipati , Sw. Banerjee ,
M. Bessner , V. Bhardwaj , D. Biswas , D. Bodrov , A. Bozek , M. Bračko ,
P. Branchini , T. E. Browder , A. Budano , M. Campajola , D. Červenkov ,
M.-C. Chang , P. Chang , B. G. Cheon , H. E. Cho , K. Cho , S.-K. Choi ,
Y. Choi , S. Choudhury , S. Das , G. De Nardo , G. De Pietro , R. Dhamija ,
F. Di Capua , J. Dingfelder , Z. Doležal , T. V. Dong , P. Ecker , D. Epifanov ,
T. Ferber , D. Ferlewicz , B. G. Fulsom , R. Garg , V. Gaur , A. Giri ,
P. Goldenzweig , E. Graziani , T. Gu , Y. Guan , K. Gudkova , C. Hadjivasiliou ,
H. Hayashii , S. Hazra , M. T. Hedges , W.-S. Hou , C.-L. Hsu , K. Inami ,
N. Ipsita , A. Ishikawa , R. Itoh , M. Iwasaki , W. W. Jacobs , S. Jia ,
Y. Jin , D. Kalita , T. Kawasaki , D. Y. Kim , K.-H. Kim , Y. J. Kim ,
Y.-K. Kim , K. Kinoshita , P. Kodyš , A. Korobov , S. Korpar , E. Kovalenko ,
P. Križan , P. Krokovny , T. Kuhr , R. Kumar , T. Kumita , A. Kuzmin ,
Y.-J. Kwon , Y.-T. Lai , T. Lam , J. S. Lange , D. Levit , L. K. Li , Y. Li ,
Y. B. Li , L. Li Gioi , J. Libby , D. Liventsev , Y. Ma , M. Masuda ,
T. Matsuda , S. K. Maurya , F. Meier , M. Merola , F. Metzner , K. Miyabayashi ,
R. Mussa , I. Nakamura , T. Nakano , M. Nakao , Z. Natkaniec , A. Natchii ,
L. Nayak , M. Nayak , S. Nishida , S. Ogawa , H. Ono , G. Pakhlova ,
S. Pardi , H. Park , J. Park , S.-H. Park , A. Passeri , S. Patra , S. Paul ,
R. Pestotnik , L. E. Piilonen , T. Podobnik , E. Prencipe , M. T. Prim , G. Russo ,
S. Sandilya , V. Savinov , G. Schnell , C. Schwanda , Y. Seino , K. Senyo ,
M. E. Sevior , W. Shan , C. Sharma , J.-G. Shiu , J. B. Singh , E. Solovieva ,
M. Starič , M. Takizawa , K. Tanida , F. Tenchini , R. Tiwary , M. Uchida ,
Y. Unno , S. Uno , P. Urquijo , Y. Usov , A. Vinokurova , S. Watanuki ,
E. Won , B. D. Yabsley , W. Yan , S. B. Yang , J. Yelton , J. H. Yin ,
Y. Yook , C. Z. Yuan , L. Yuan , Y. Yusa , Z. P. Zhang , and V. Zhilich

(The Belle Collaboration)

(Dated: March 6, 2024)

Abstract

Using the data samples of 102 million $\Upsilon(1S)$ and 158 million $\Upsilon(2S)$ events collected by the Belle detector, we search for a pentaquark state in the pJ/ψ final state from $\Upsilon(1, 2S)$ inclusive decays. Here, the charge-conjugate $\bar{p}J/\psi$ is included. We observe clear pJ/ψ production in $\Upsilon(1, 2S)$ decays and measure the branching fractions to be $\mathcal{B}[\Upsilon(1S) \rightarrow pJ/\psi + anything] = [4.27 \pm 0.16(stat.) \pm 0.20(syst.)] \times 10^{-5}$ and $\mathcal{B}[\Upsilon(2S) \rightarrow pJ/\psi + anything] = [3.59 \pm 0.14(stat.) \pm 0.16(syst.)] \times 10^{-5}$. We also measure the cross section of inclusive pJ/ψ production in e^+e^- annihilation to be $\sigma(e^+e^- \rightarrow pJ/\psi + anything) = [57.5 \pm 2.1(stat.) \pm 2.5(syst.)]$ fb at $\sqrt{s} = 10.52$ GeV using an 89.5 fb^{-1} continuum data sample. There is no significant $P_c(4312)^+$, $P_c(4440)^+$ or $P_c(4457)^+$ signal found in the pJ/ψ final states in $\Upsilon(1, 2S)$ inclusive decays. We determine the upper limits of $\mathcal{B}[\Upsilon(1, 2S) \rightarrow P_c^+ + anything] \cdot \mathcal{B}(P_c^+ \rightarrow pJ/\psi)$ to be at the 10^{-6} level.

PACS numbers: 14.40.Gx, 13.25.Gv, 13.66.Bc

I. INTRODUCTION

In the conventional quark model, a hadron is either a meson containing a quark and an anti-quark or an (anti-)baryon containing three (anti-)quarks. However, the fundamental theory of strong interaction, Quantum Chromodynamics, does not forbid new structures of hadrons beyond the conventional quark model, such as glueball states containing only gluons, hybrid states containing gluons and quarks, or multi-quark states containing more than three quarks [1]. Many theoretical and experimental efforts have been devoted to predicting and searching for these exotic states [2, 3]. In 2003, the Belle experiment observed the $X(3872)$ in $B \rightarrow K + \pi^+ \pi^- J/\psi$ decay [4], which was the clearest evidence yet of the existence of exotic states. Five years later, Belle observed the $Z(4430)^+$ in the decay $B \rightarrow K + \pi^+ \psi(2S)$ [5]. The $c\bar{c}$ component and the non-zero net charge of the final state $\pi^+ \psi(2S)$ indicate that the $Z(4430)^+$ is a good candidate for a tetraquark state. Since then, many candidate multi-quark states have been observed by the Belle, LHCb, and BESIII experiments [6–13]. In the pentaquark sector, the LHCb experiment discovered $P_c(4380)^+$ and $P_c(4450)^+$ in the decay $\Lambda_b \rightarrow K + p J/\psi$ [14], but an updated analysis using ten times the statistics divided the structures into three states [15], the $P_c(4312)^+$, $P_c(4440)^+$ and $P_c(4457)^+$. The deuteron can be considered a candidate for a hexaquark state [16]. The observations of deuterons in the $\Upsilon(nS)$ inclusive decays by the ARGUS, CLEO, and BaBar experiments provide clues of searching for more candidates of multi-quark states in the $\Upsilon(nS)$ inclusive decays [17–19].

The Belle experiment collected the world’s largest $\Upsilon(1, 2S)$ data samples in the last years of data taking. The $\Upsilon(1S)$ data sample with an integrated luminosity $\mathcal{L}_{\Upsilon(1S)} = 5.8 \text{ fb}^{-1}$ contains $(102 \pm 2) \times 10^6$ $\Upsilon(1S)$ events [20], while the $\Upsilon(2S)$ data sample has $\mathcal{L}_{\Upsilon(2S)} = 24.7 \text{ fb}^{-1}$ and $(158 \pm 4) \times 10^6$ $\Upsilon(2S)$ events [21]. Using the two data samples, we search for a P_c^+ state in the inclusive production of pJ/ψ final states via $\Upsilon(1, 2S)$ decays. Here and hereinafter, P_c^+ is $P_c(4312)^+$, $P_c(4440)^+$, or $P_c(4457)^+$. The charge-conjugated final state $P_c^- \rightarrow \bar{p}J/\psi$ is included throughout this study. We also use a Belle continuum data sample with an integrated luminosity of $\mathcal{L}_{\text{cont}} = 89.5 \text{ fb}^{-1}$ taken at center-of-mass (c.m.) energy $\sqrt{s} = 10.52 \text{ GeV}$ [60 MeV below the peak of the $\Upsilon(4S)$ resonance] to investigate the pJ/ψ final state from continuum productions, which could be backgrounds in the $\Upsilon(1, 2S)$ data samples for studying the $\Upsilon(1, 2S)$ decays.

II. THE BELLE DETECTOR AND MONTE CARLO SIMULATION

The Belle detector is a large-solid-angle magnetic spectrometer [22]. It consists of several subdetectors, including a silicon vertex detector, a central drift chamber with 50 layers, an array of aerogel threshold Cherenkov counters, a barrel-like arrangement of time-of-flight scintillation counters, and an electromagnetic calorimeter (ECL) comprised of CsI(Tl) crystals. All the above are located within a superconducting solenoid coil which generates a magnetic field of 1.5 T. An iron flux return outside the coil is instrumented to detect K_L^0 mesons and identify muons. The origin of the coordinate system is defined as the position of the nominal interaction point. The z axis is aligned with the direction opposite to the e^+ beam and points along the magnetic field within the solenoid. The x axis points horizontally outwards of the storage ring, and the y axis is vertically upwards. The angles of the polar (θ) and azimuthal (ϕ) are measured relative to the positive z axis.

To optimize the selection criteria, we use EvtGen to simulate signal Monte Carlo (MC) samples of $\Upsilon(1, 2S) \rightarrow P_c^+ + \bar{p} + q\bar{q}$ with $P_c^+ \rightarrow pJ/\psi$ according to three-body phase space [23],

where $q\bar{q}$ ($q = u, d, s, c$) is a quark-antiquark pair of random flavor whose hadronization is simulated by PYTHIA6.4 [24]. Each P_c^+ MC sample has 2×10^4 events, and we combine the three P_c^+ signal MC samples for the selection criteria optimization. To study the efficiency and mass resolution of the pJ/ψ invariant mass ($M_{pJ/\psi}$), we generate efficiency MC samples of P_c^+ , whose mass is fixed to different values from $4.1 \text{ GeV}/c^2$ to $5.0 \text{ GeV}/c^2$, and the width is set to zero. To study pJ/ψ production not due to P_c^+ decays, we generate a no- P_c^+ MC sample of $\Upsilon(1, 2S) \rightarrow J/\psi + p + \bar{p} + q\bar{q}$ according to four-body phase space [23]. To simulate the hadronization of $q\bar{q}$, we define a state of $X \rightarrow q\bar{q}$ where X has a mass of $2.6 \text{ GeV}/c^2$ and a width of 2.7 GeV in $\Upsilon(1S)$ decays; similarly a mass of $3.2 \text{ GeV}/c^2$ and width of 3.3 GeV in $\Upsilon(2S)$ decays. We simulate the geometry and the response of the Belle detector using a GEANT3-based MC technique [25].

III. EVENT SELECTION

To reconstruct the pJ/ψ final state, we select events with at least three well-measured charged tracks. Two tracks with opposite charges are chosen as candidates for J/ψ decaying into e^+e^- (called the e^+e^- mode) or $\mu^+\mu^-$ (called the $\mu^+\mu^-$ mode). A well-measured charged track has impact parameters of $dr < 0.5 \text{ cm}$ in the $r - \phi$ plane and $|dz| < 5 \text{ cm}$ in the $r - z$ plane with respect to the interaction point, and a transverse momentum larger than $0.1 \text{ GeV}/c$. For each charged track, we combine information from subdetectors of Belle to form a likelihood \mathcal{L}_i for each putative particle species (i) [26]. We form the likelihood ratios $\mathcal{R}_e \equiv \mathcal{L}_e/(\mathcal{L}_e + \mathcal{L}_{\text{hadrons}})$ and $\mathcal{R}_\mu \equiv \mathcal{L}_\mu/(\mathcal{L}_\mu + \mathcal{L}_{\text{hadrons}})$ for electron and muon identifications [27, 28]. For electrons from $J/\psi \rightarrow e^+e^-$ decay, we require both tracks to have $\mathcal{R}_e > 0.9$ and include the bremsstrahlung photons detected in the ECL within 0.05 radians of the original e^+ or e^- direction in calculating the $e^+e^-(\gamma)$ invariant mass. For muons from $J/\psi \rightarrow \mu^+\mu^-$ decay, we require both tracks to have $\mathcal{R}_\mu > 0.9$. The single lepton identification efficiency is $(93.9 \pm 0.2)\%$ in the e^+e^- mode and $(91.9 \pm 0.2)\%$ in the $\mu^+\mu^-$ mode. We identify a track with $\mathcal{R}_{p/K} = \frac{\mathcal{L}_p}{\mathcal{L}_p + \mathcal{L}_K} > 0.6$ and $\mathcal{R}_{p/\pi} = \frac{\mathcal{L}_p}{\mathcal{L}_p + \mathcal{L}_\pi} > 0.6$ as a proton. The efficiency of proton identification is $(97.3 \pm 0.1)\%$. To remove backgrounds from $\Lambda \rightarrow p\pi$ decay in the proton selection, we reconstruct all the pion candidates with $\mathcal{R}_{\pi/K} = \mathcal{L}_\pi/(\mathcal{L}_\pi + \mathcal{L}_K) > 0.6$ and a charge opposite to that of the proton. We remove the proton candidate if it is part of any $p\pi$ combination of mass $1.105 \text{ GeV}/c^2 < M_{p\pi} < 1.12 \text{ GeV}/c^2$, where $M_{p\pi}$ is the invariant mass of the $p\pi$ combination. Furthermore, to remove the proton candidates from beam backgrounds, we require the difference of the dz parameter for p and ℓ^\pm to be $|\Delta dz| < 0.5 \text{ cm}$.

The $\Upsilon(1, 2S)$ data samples, and the continuum data sample, all show clear J/ψ signals in both the e^+e^- mode and the $\mu^+\mu^-$ mode. Figure 1 shows the invariant-mass distributions of the lepton pair ($M_{\ell^+\ell^-}$), which is the sum of the e^+e^- mode and the $\mu^+\mu^-$ mode, in the $\Upsilon(1, 2S)$ data samples. Fitting the $M_{\ell^+\ell^-}$ distributions using a Gaussian function for the J/ψ signal and a second-order Chebychev function for the backgrounds, we get the mass resolution of the J/ψ signal to be $8.7 \pm 0.6 \text{ MeV}/c^2$ ($10.1 \pm 0.5 \text{ MeV}/c^2$) in the $\Upsilon(1S)$ [$\Upsilon(2S)$] data sample and $8.2 \pm 0.1 \text{ MeV}/c^2$ ($8.6 \pm 0.1 \text{ MeV}/c^2$) in the signal MC simulation of $\Upsilon(1S)$ [$\Upsilon(2S)$] decays. We define the J/ψ signal region to be $|M_{\ell^+\ell^-} - m_{J/\psi}| < 3\sigma$, where $m_{J/\psi}$ is the nominal mass of J/ψ [29] and $\sigma = 10 \text{ MeV}/c^2$. To estimate the backgrounds to the J/ψ , we define the J/ψ mass sideband regions as $|M_{\ell^+\ell^-} - m_{J/\psi} \pm 9\sigma| < 3\sigma$.

Figures 2(a) and 2(b) show the distributions of the recoil mass squared against the pJ/ψ system in $\Upsilon(1, 2S)$ data samples and signal MC simulations. This quantity is calculated

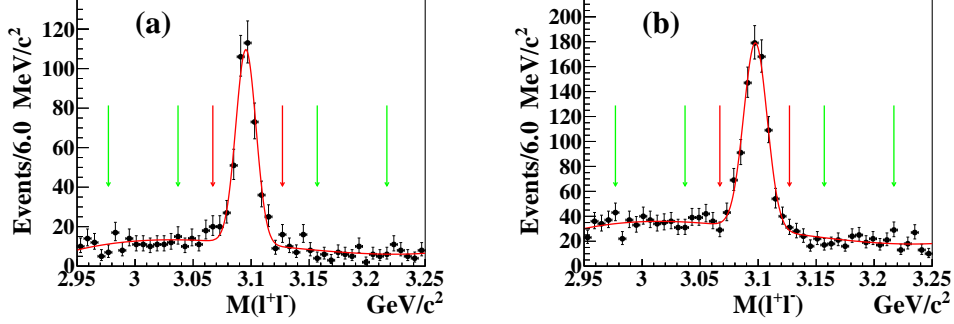


FIG. 1. The invariant-mass distributions of the lepton pair from (a) the $\Upsilon(1S)$ data sample and (b) the $\Upsilon(2S)$ data sample. The curves show the best fit results with a Gaussian function for the J/ψ signal and a second-order Chebychev function for the backgrounds. The red arrows indicate the J/ψ signal region and the green ones indicate the J/ψ mass sideband regions.

by $M_{\text{recoil}}^2(pJ/\psi) \equiv (P_{e^+e^-} - P_{J/\psi})^2$, where $P_{e^+e^-}$ is the 4-momentum of the e^+e^- collision and $P_{pJ/\psi}$ is the 4-momentum of the pJ/ψ combination. In data, there are accumulations between $-5 \text{ GeV}^2/c^4$ and $5 \text{ GeV}^2/c^4$ for the events selected in the J/ψ signal region and these can be described well with the backgrounds estimated from the J/ψ mass sideband regions. These backgrounds appear in the e^+e^- mode but are scarce in the $\mu^+\mu^-$ mode. On the other hand, these events produce a large peak at zero and a wide distribution of the recoil mass squared against the J/ψ candidate, calculated by $M_{\text{recoil}}^2(J/\psi) \equiv (P_{e^+e^-} - P_{J/\psi})^2$, where $P_{J/\psi}$ is the 4-momentum of the J/ψ candidate. They are identified as backgrounds from Bhabha events with high energy bremsstrahlung radiation photon(s) and an additional proton from beam backgrounds. As this proton is not from an e^+e^- collision, this background can produce negative accumulations in the $M_{\text{recoil}}^2(pJ/\psi)$ distributions. We require $M_{\text{recoil}}^2(pJ/\psi) > 10 \text{ GeV}^2/c^4$ to suppress these backgrounds with a selection efficiency of about 99% in $\Upsilon(1, 2S)$ decays. Figures 2(c) and 2(d) show the distributions of $M_{\text{recoil}}^2(J/\psi)$ after this requirement. We notice that the data have higher distributions than signal MC simulations in the region $M_{\text{recoil}}^2(J/\psi) < 30 \text{ GeV}^2/c^4$. In the range $M_{\text{recoil}}^2(J/\psi) > 30 \text{ GeV}^2/c^4$, the MC and the data are in good agreement in $\Upsilon(1S)$, but the MC is slightly higher than the data in $\Upsilon(2S)$. It is also interesting to see an enhancement at around $22 \text{ GeV}^2/c^4$ in the $\Upsilon(1S)$ decays. However, the statistics are too limited to draw any conclusions with the presently available dataset.

IV. INVARIANT MASS SPECTRA OF pJ/ψ

All the candidates satisfying the selection criteria described above are accepted, including p or \bar{p} with the same J/ψ candidate or multiple candidates sharing one lepton. We show the momentum distributions of the p/\bar{p} after selection criteria in Fig. 3.

According to the efficiency MC simulations, we obtain an efficiency varying from 29% (26%) to 36% (33%) in the $\Upsilon(1S)$ [$\Upsilon(2S)$] decays, and the mass resolution increasing from $1.5 \text{ MeV}/c^2$ to $4.9 \text{ MeV}/c^2$ for $M_{pJ/\psi} \in [4.1, 5.0] \text{ GeV}/c^2$. We notice that the width of $P_c(4457)^+$ reported by LHCb is $\Gamma_{P_c(4457)^+} = 6.4 \pm 2.0_{-1.9}^{+5.7} \text{ MeV}$ [15] and the mass resolution near the mass of $P_c(4457)^+$ is about $3.0 \text{ MeV}/c^2$. Therefore, we need to consider the mass resolution in fitting the $M_{pJ/\psi}$ distributions for the possible P_c^+ signals. Here and hereinafter,

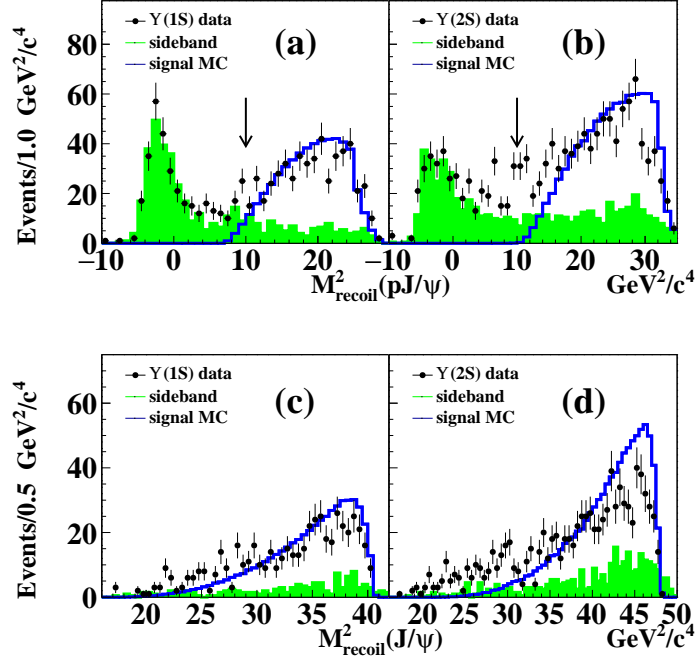


FIG. 2. The distributions of the recoil mass squared of pJ/ψ (upper), and J/ψ (lower) in $\Upsilon(1S)$ (left) and $\Upsilon(2S)$ (right) decays. The dots with error bars are data, the shaded histograms are backgrounds estimated from the J/ψ mass sideband regions, and the solid histograms are signal MC simulations. The arrows show the requirement $M_{\text{recoil}}^2(pJ/\psi) > 10 \text{ GeV}^2/c^4$.

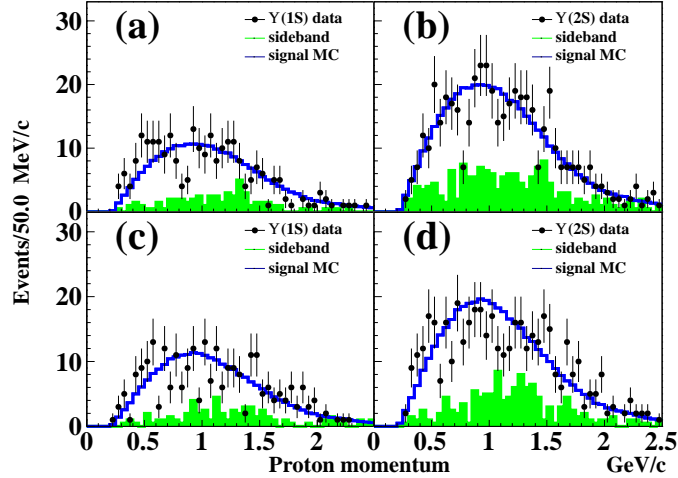


FIG. 3. The momentum distributions of p/\bar{p} in $\Upsilon(1,2S)$ inclusive decays. The first row is the momenta of p and the second of \bar{p} . The left and right panels are $\Upsilon(1S)$ and $\Upsilon(2S)$, respectively. The dots with error bars are data, the shaded histograms are backgrounds estimated from the J/ψ mass sideband regions, and the solid histograms are signal MC simulations.

TABLE I. The mass resolution, the ratio of the number of P_c^+ signals to the number of all pJ/ψ combinations, and the efficiency of all the pJ/ψ combinations from the signal MC simulations of $P_c(4312)^+$, $P_c(4440)^+$, and $P_c(4457)^+$ in $\Upsilon(1, 2S)$ decays.

—	$\Upsilon(1S)$ decays			$\Upsilon(2S)$ decays		
	$P_c(4312)^+$	$P_c(4440)^+$	$P_c(4457)^+$	$P_c(4312)^+$	$P_c(4440)^+$	$P_c(4457)^+$
mass resolution (MeV/ c^2)	2.9 ± 0.1	3.2 ± 0.2	3.4 ± 0.1	2.8 ± 0.1	3.0 ± 0.2	3.2 ± 0.1
Ratio of $N_{P_c^+}/N_{pJ/\psi}$	0.60	0.56	0.57	0.59	0.56	0.54
$\varepsilon_{\text{allcmb}}^{\text{MC}}$ (%)	58.7 ± 0.1	59.2 ± 0.1	59.7 ± 0.1	58.9 ± 0.1	59.2 ± 0.1	59.5 ± 0.1

the first uncertainty quoted is statistical, while the second corresponds to the total systematic uncertainty.

We then study the $M_{pJ/\psi}$ distributions from the signal MC simulations of $P_c(4312)^+$, $P_c(4440)^+$, and $P_c(4457)^+$. In each distribution, there is a clear P_c^+ peak and a plateau of wrong combination with particle(s) from the recoil of P_c^+ . We perform a fit to this distribution using a Breit-Wigner function convolved with a Gaussian resolution function to describe the signals and a first-order polynomial function to describe the plateau of the wrong combinations. The fit range is $M_{P_c^+} \pm 200$ MeV/ c^2 , where $M_{P_c^+}$ is the mass of P_c^+ . The fits yield mass resolutions of around 3 MeV/ c^2 for each P_c^+ state. The mass resolutions obtained here agree with those obtained from the efficiency MC simulations directly. We calculate the ratio $\mathcal{R} \equiv N_{P_c^+}/N_{pJ/\psi}$ to be approximately 0.6, where the $N_{P_c^+}$ and $N_{pJ/\psi}$ are the number of P_c^+ signals from the fit and the number of all pJ/ψ combinations being selected between 4.0 GeV/ c^2 and 5.0 GeV/ c^2 , respectively. The efficiencies of all combinations ($\varepsilon_{\text{allcmb}}^{\text{MC}}$) are about 60%. We list the details of the mass resolutions, the ratios \mathcal{R} , and the efficiencies $\varepsilon_{\text{allcmb}}^{\text{MC}}$ from the signal MC simulations of $P_c(4312)^+$, $P_c(4440)^+$, and $P_c(4457)^+$ in $\Upsilon(1, 2S)$ inclusive decays in Table I.

We study the $M_{pJ/\psi}$ distributions obtained from the $\Upsilon(1S)$, $\Upsilon(2S)$, and continuum data samples, and show them in Figs. 4(a-d), 4(e-h), and 4(i-l), respectively. There are clear pJ/ψ signals in the three data samples. As mentioned, we use the distributions obtained from the continuum data sample to estimate the backgrounds from e^+e^- annihilation in the $\Upsilon(1, 2S)$ decays. For this, we scale the luminosities and correct for the efficiencies and the c.m. energy dependence of the Quantum Electrodynamics (QED) cross section $\sigma_{e^+e^-} \propto 1/s$, resulting in scale factors $f_{\text{scale}} = (\mathcal{L}_{\Upsilon(1,2S)} \times \varepsilon_{\Upsilon(1,2S)} \times s_{\text{cont}})/(\mathcal{L}_{\text{cont}} \times \varepsilon_{\text{cont}} \times s_{\Upsilon(1,2S)}) = 0.077$ and 0.301 for $\Upsilon(1S)$ and $\Upsilon(2S)$, respectively. We find no peaking component in the combined $M_{pJ/\psi}$ distribution from Figs 4(i-l) and obtain the number of pJ/ψ candidates to be $N_{\text{cont}}^{pJ/\psi} = 383 \pm 20$ after subtracting the backgrounds estimated from the J/ψ mass sideband regions. To estimate the backgrounds due to the mis-identification of proton, we replace the proton identification requirements with $\mathcal{L}_p/(\mathcal{L}_p + \mathcal{L}_K) < 0.4$ or $\mathcal{L}_p/(\mathcal{L}_p + \mathcal{L}_\pi) < 0.4$ in the signal selection. We obtain 1746 ± 42 $K^\pm J/\psi$ signals with kaon identification efficiency of 93.5% or 1710 ± 41 $\pi^\pm J/\psi$ signals with pion identification efficiency of 92.4%. Taking into account mis-identification rates, we expect the number of backgrounds from $K^\pm J/\psi$ or $\pi^\pm J/\psi$ to be $50.3 \pm 0.9 \pm 1.3$, where the systematic uncertainty is described in Sec. V. Hence, the number of pJ/ψ events after all background subtractions is found to be $N_{\text{cont}}^{pJ/\psi} = 333 \pm 18$. With the scale factor f_{scale} , we expect $26 \pm 2 \pm 1$ and $100 \pm 5 \pm 4$ pJ/ψ signals from e^+e^- annihilation in the $\Upsilon(1S)$ and $\Upsilon(2S)$ data samples, respectively.

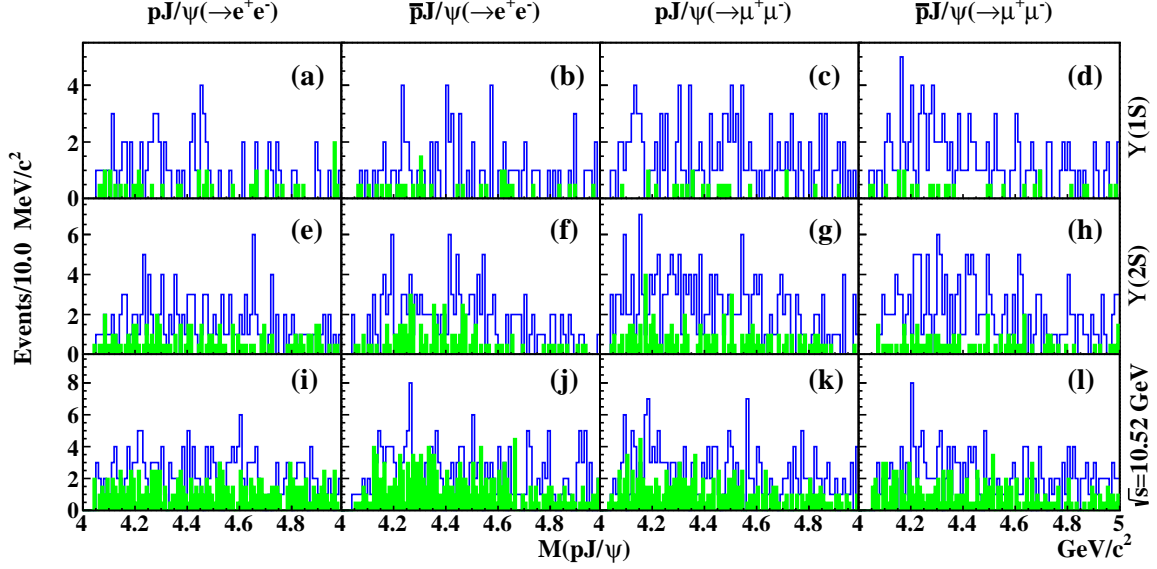


FIG. 4. The invariant-mass distributions of pJ/ψ in the $\Upsilon(1S)$, $\Upsilon(2S)$, and continuum data samples. From left to right, the four panels are $p + J/\psi$ in e^+e^- mode, $\bar{p} + J/\psi$ in e^+e^- mode, $p + J/\psi$ in $\mu^+\mu^-$ mode, and $\bar{p} + J/\psi$ in $\mu^+\mu^-$ mode. From top to bottom, the three rows are the $\Upsilon(1S)$ decays, the $\Upsilon(2S)$ decays, and the continuum productions at $\sqrt{s} = 10.52$ GeV. The solid histograms are the pJ/ψ signals, and the shaded histograms are backgrounds estimated from the J/ψ mass sideband regions.

We use the $N_{\text{cont}}^{pJ/\psi}$ obtained from the continuum data sample to calculate the cross section of the inclusive pJ/ψ production in e^+e^- annihilation via

$$\sigma(e^+e^- \rightarrow pJ/\psi + \text{anything}) = \frac{N_{\text{cont}}^{pJ/\psi}}{L_{\text{cont}} \times \varepsilon_{\text{cont}}^{\text{no}P_c} \times \mathcal{B}(J/\psi \rightarrow \ell^+\ell^-) \times (1 + \delta_{\text{ISR}})}. \quad (1)$$

Here, $\varepsilon_{\text{cont}}^{\text{no}P_c} = 66.1\%$ is the efficiency obtained from no- P_c^+ MC simulation of continuum production, $(1 + \delta_{\text{ISR}}) = 0.82$ is the radiative correction factor [30, 31], and $\mathcal{B}(J/\psi \rightarrow \ell^+\ell^-) = (11.93 \pm 0.07)\%$ is the branching fraction of J/ψ decaying to e^+e^- or $\mu^+\mu^-$ [29]. We obtain the cross section $\sigma(e^+e^- \rightarrow pJ/\psi + \text{anything}) = (57.5 \pm 2.1 \pm 2.5)$ fb at $\sqrt{s} = 10.52$ GeV, where the systematic uncertainties are discussed in Sec. V.

Figure 5 shows the combined distributions of Figs. 4(a-d) and 4(e-h) for $\Upsilon(1S)$ and $\Upsilon(2S)$ inclusive decays, respectively. Since we measure the pJ/ψ production in $\Upsilon(1, 2S)$ inclusive decays, the background of continuum production in Fig. 5 is removed. We estimate the number of backgrounds from $K^\pm J/\psi$ or $\pi^\pm J/\psi$ to be 17.9 ± 1.2 (43.9 ± 3.0) in $\Upsilon(1S)$ [$\Upsilon(2S)$] decays. With the backgrounds estimated from the J/ψ mass sidebands and those from mis-identification of proton being subtracted, we get the final numbers of pJ/ψ signal events to be $N_{\Upsilon(1S)}^{pJ/\psi} = 363 \pm 19$ in the $\Upsilon(1S)$ decays and $N_{\Upsilon(2S)}^{pJ/\psi} = 541 \pm 23$ in the $\Upsilon(2S)$ decays. These yields are much higher than those estimated to be due to the underlying e^+e^- continuum production. To measure the production of pJ/ψ in $\Upsilon(1, 2S)$ inclusive decays, we use the no- P_c^+ MC samples to estimate the efficiencies to be $\varepsilon_{\Upsilon(1,2S)}^{\text{no}P_c} = 64.8\%$ and 65.1% for the $\Upsilon(1S)$ and $\Upsilon(2S)$ inclusive decays in the region of $4.0 \text{ GeV}/c^2 < M_{pJ/\psi} < 5.5 \text{ GeV}/c^2$.

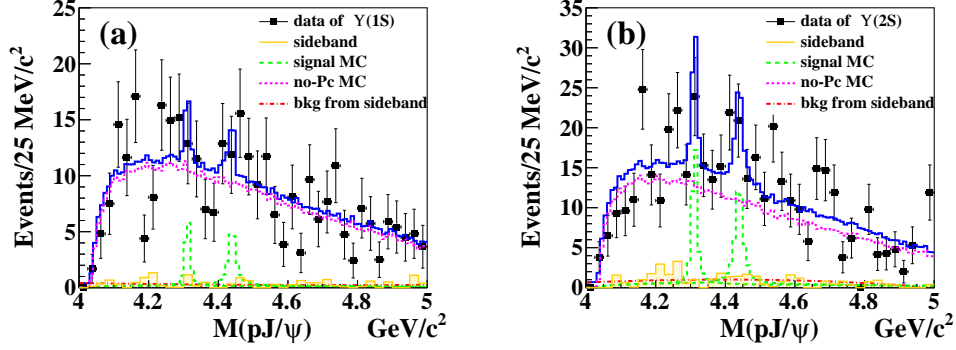


FIG. 5. The combined distributions of the invariant masses of pJ/ψ and $\bar{p}J/\psi$ from (a) the $\Upsilon(1S)$ inclusive decays and (b) the $\Upsilon(2S)$ inclusive decays, and the fit results including $P_c(4312)^+$, $P_c(4440)^+$ and $P_c(4457)^+$. The dots with error bars are data. The shaded histograms are the backgrounds estimated from the J/ψ mass sidebands. The blue histograms are the best fit results; the green histograms are the $P_c(4312)^+$, $P_c(4440)^+$, and $P_c(4457)^+$ components; the pink histograms are the no- P_c^+ components.

We calculate the branching fractions of $\Upsilon(1, 2S)$ inclusive decays using

$$\mathcal{B}[\Upsilon(1, 2S) \rightarrow pJ/\psi + \text{anything}] = \frac{N_{\Upsilon(1,2S)}^{pJ/\psi} - f_{\text{scale}} \times N_{\text{cont}}^{pJ/\psi}}{N_{\Upsilon(1,2S)} \times \varepsilon_{\Upsilon(1,2S)}^{\text{no}P_c} \times \mathcal{B}(J/\psi \rightarrow \ell^+ \ell^-)}, \quad (2)$$

where $N_{\Upsilon(1,2S)}$ are the numbers of $\Upsilon(1, 2S)$ events in the $\Upsilon(1, 2S)$ data samples. We obtain that $\mathcal{B}[\Upsilon(1S) \rightarrow pJ/\psi + \text{anything}] = (4.27 \pm 0.16 \pm 0.20) \times 10^{-5}$ and $\mathcal{B}[\Upsilon(2S) \rightarrow pJ/\psi + \text{anything}] = (3.59 \pm 0.14 \pm 0.16) \times 10^{-5}$ for the first time. Excluding the background of $\Upsilon(2S) \rightarrow \Upsilon(1S) + \text{anything}$ transitions and $\Upsilon(1S) \rightarrow pJ/\psi + \text{anything}$ with this measurement of $\mathcal{B}[\Upsilon(1S) \rightarrow pJ/\psi + \text{anything}]$, we correct the $\mathcal{B}[\Upsilon(2S) \rightarrow pJ/\psi + \text{anything}]$ and find a value of $(2.46 \pm 0.15 \pm 0.17) \times 10^{-5}$. Systematic uncertainties are listed in Table III, which is described in Sec. V. The world average values of the branching fractions of J/ψ production in $\Upsilon(1, 2S)$ decays are $\mathcal{B}[\Upsilon(1S) \rightarrow J/\psi + \text{anything}] = (5.4 \pm 0.4) \times 10^{-4}$ and $\mathcal{B}[\Upsilon(2S) \rightarrow J/\psi + \text{anything}] < 6 \times 10^{-3}$ at 90% credibility [29]. Thus, the ratio $\mathcal{B}(\Upsilon \rightarrow pJ/\psi + \text{anything})/\mathcal{B}(\Upsilon \rightarrow J/\psi + \text{anything})$ is of order $10^{-1} - 10^{-2}$ in $\Upsilon(1, 2S)$ decays.

To estimate the production of a possible P_c^+ state in the $\Upsilon(1S)$ or $\Upsilon(2S)$ inclusive decays, we perform binned maximum likelihood fits to the distribution of $M_{pJ/\psi}$ in Fig. 5(a) or 5(b) with

$$f_{\text{PDF}} = f_{P_c(4312)^+} + f_{P_c(4440)^+} + f_{P_c(4457)^+} + f_{\text{no}P_c} + f_{\text{bkg}}, \quad (3)$$

where $f_{P_c(4312)^+}$, $f_{P_c(4440)^+}$, $f_{P_c(4457)^+}$, and $f_{\text{no}P_c}$ are the histogram PDFs obtained from the signal MC simulations on $P_c(4312)^+$, $P_c(4440)^+$, $P_c(4457)^+$, and the no- P_c^+ MC simulation. We use a second-order polynomial function for the f_{bkg} to describe the backgrounds due to J/ψ selection. We fit to the events from the J/ψ signal region with f_{PDF} and the events from J/ψ mass sidebands with f_{bkg} simultaneously. The fit yields the numbers of P_c^+ signals [$N_{\text{fit}}^A(P_c^+)$], as listed in Table II. Since none of the $P_c(4312)^+$, $P_c(4440)^+$, or $P_c(4457)^+$ is significant, we integrate the likelihood versus the $N_{\text{fit}}^A(P_c^+)$ and determine the upper limits $N_{\text{fit}}^{\text{A,UL}}(P_c^+)$ at 90% credibility. We also perform a fit to the $M_{pJ/\psi}$ distribution in Fig. 5(a)

TABLE II. The fit results and the upper limits of $P_c(4312)^+$, $P_c(4440)^+$, and $P_c(4457)^+$ productions in $\Upsilon(1, 2S)$ inclusive decays. $N_{\text{fit}}^{\text{A}}$ is the number of P_c^+ signals in the fit with the PDF function f_{PDF} contains $P_c(4312)^+$, $P_c(4440)^+$, and $P_c(4457)^+$ states, and $N_{\text{fit}}^{\text{A,UL}}$ is the related upper limits at 90% credibility. $N_{\text{fit}}^{\text{B}}$ is the number of P_c^+ signals in the fit with the PDF function that contains only a single P_c^+ state, and $N_{\text{fit}}^{\text{B,UL}}$ is the related upper limits at 90% credibility. $N_{\text{sig}}^{\text{UL}}$ is the final conservative estimation of the upper limit of the number of P_c^+ signals in $\Upsilon(1, 2S)$ inclusive decays. \mathcal{B}^{UL} is the upper limit of $\mathcal{B}(\Upsilon \rightarrow P_c^+ + \text{anything}) \cdot \mathcal{B}(P_c^+ \rightarrow pJ/\psi)$ at 90% credibility.

—	$\Upsilon(1S)$ decays			$\Upsilon(2S)$ decays		
	$P_c(4312)^+$	$P_c(4440)^+$	$P_c(4457)^+$	$P_c(4312)^+$	$P_c(4440)^+$	$P_c(4457)^+$
$N_{\text{fit}}^{\text{A}}$	10 ± 8	14 ± 12	-3 ± 9	30 ± 16	33 ± 15	0 ± 3
$N_{\text{fit}}^{\text{A,UL}}$	26	37	14	52	60	6
$N_{\text{fit}}^{\text{B}}$	10 ± 8	12 ± 11	3 ± 9	29 ± 12	31 ± 15	0 ± 3
$N_{\text{fit}}^{\text{B,UL}}$	26	33	17	50	57	7
$N_{\text{sig}}^{\text{UL}}$	31	47	34	56	77	26
$\mathcal{B}^{\text{UL}} (\times 10^{-6})$	4.5	6.8	4.9	5.3	7.2	2.4

or 5(b) with individual P_c^+ state in the f_{PDF} , which yields the new number of P_c^+ signal [$N_{\text{fit}}^{\text{B}}(P_c^+)$]. Similarly, we determine the related upper limits $N_{\text{fit}}^{\text{B,UL}}(P_c^+)$ for $P_c(4312)^+$, $P_c(4440)^+$, and $P_c(4457)^+$ at 90% credibility. We also estimate the upper limits by varying the masses and widths of P_c^+ states by 1σ in these tests. We take the largest values of the upper limits as the conservative estimations of the upper limits of the numbers of the P_c^+ signals [$N_{\text{sig}}^{\text{UL}}(P_c^+)$] in $\Upsilon(1, 2S)$ inclusive decays. We then calculate the upper limit of the branching fraction of a P_c^+ state produced in $\Upsilon(1S)$ [$\Upsilon(2S)$] inclusive decays at 90% credibility with

$$\mathcal{B}[\Upsilon(1, 2S) \rightarrow P_c^+ + \text{anything}] \cdot \mathcal{B}(P_c^+ \rightarrow pJ/\psi) < \frac{N_{\text{sig}}^{\text{UL}}(P_c^+)}{N_{\Upsilon(1,2S)} \cdot \varepsilon_{\text{allcmb}}^{\text{MC}} \cdot \mathcal{B}(J/\psi \rightarrow \ell^+ \ell^-) (1 - \delta_{\text{sys}})}, \quad (4)$$

where $\delta_{\text{sys}} = 5.0\%$ (4.7%) is the systematic uncertainty of $\Upsilon(1S)$ [$\Upsilon(2S)$] decays, which are described in Sec. V. We summarize the values of $N_{\text{fit}}^{\text{A}}(P_c^+)$, $N_{\text{fit}}^{\text{A,UL}}(P_c^+)$, $N_{\text{fit}}^{\text{B}}(P_c^+)$, $N_{\text{fit}}^{\text{B,UL}}(P_c^+)$, $N_{\text{sig}}^{\text{UL}}(P_c^+)$, and the upper limit of $\mathcal{B}[\Upsilon(1, 2S) \rightarrow P_c^+ + \text{anything}] \cdot \mathcal{B}(P_c^+ \rightarrow pJ/\psi)$ at 90% credibility in Table II.

V. SYSTEMATIC UNCERTAINTIES

As listed in Table III, we consider the following systematic uncertainties in determining the branching fractions $\mathcal{B}[\Upsilon(1, 2S) \rightarrow pJ/\psi + \text{anything}]$ and measuring $\sigma(e^+e^- \rightarrow pJ/\psi + \text{anything})$ at $\sqrt{s} = 10.52$ GeV: particle identification, tracking efficiency, J/ψ signal region, $M_{\text{recoil}}^2(pJ/\psi)$ requirement, branching fraction of J/ψ decay, number of $\Upsilon(1, 2S)$ events, integrated luminosity, modeling in MC simulation, and statistics of MC samples, etc. The uncertainties due to the lepton identification are 2.0% and 0.5% for e^\pm and μ^\pm , respectively. For the proton identification, we have applied an efficiency correction according to the momentum and angle in the laboratory frame. Shifting the correction factor by 1σ , we get the related efficiency difference of 0.43% and take 0.5% to be the systematic uncertainty

TABLE III. The summary of the systematic uncertainties (%) in the measurements of $\mathcal{B}[\Upsilon(1, 2S) \rightarrow pJ/\psi + \text{anything}]$ and $\sigma(e^+e^- \rightarrow pJ/\psi + \text{anything})$ at $\sqrt{s} = 10.52$ GeV.

Source	$\Upsilon(1S)$ decay	$\Upsilon(2S)$ decay	$\sigma(e^+e^- \rightarrow pJ/\psi + \text{anything})$
Particle identification	2.1	2.1	2.1
Tracking	1.1	1.1	1.1
J/ψ signal region	0.6	0.5	0.4
$M_{\text{recoil}}^2(pJ/\psi)$ requirement	1.5	1.5	1.5
$\mathcal{B}(J/\psi \rightarrow \ell^+\ell^-)$	0.6	0.6	0.6
$1 + \delta_{\text{ISR}}$	—	—	1.0
Modeling in MC simulation	2.8	2.3	2.6
Number of $\Upsilon(1, 2S)$ events	2.2	2.3	—
Integrated luminosity	—	—	1.4
Statistics of MC samples	0.5	0.5	0.5
Sum in quadrature	4.6	4.4	4.3

of proton identification. Therefore, the total systematic uncertainty due to the particle identification is 2.1%. In estimating the backgrounds from KJ/ψ or $\pi J/\psi$, the mis-identification of $K(\pi)$ to p is $(1.98 \pm 0.07)\%$ [$(0.72 \pm 0.02)\%$]. The uncertainties of mis-identification are not listed in Table III but contribute 0.4, 1.1, 1.3 in the numbers of estimated backgrounds from KJ/ψ and $\pi J/\psi$ in $\Upsilon(1S)$ decays, $\Upsilon(2S)$ decays, and continuum productions. The uncertainty due to the tracking efficiency is 0.35% per track and adds linearly. Fitting the $M_{\ell+\ell}$ -distributions from data and MC simulations with a Gaussian function for J/ψ signal and a second-order Chebychev function for backgrounds, we obtain the efficiencies of J/ψ mass signal window to be $\varepsilon_{J/\psi}^{\text{data}} = (99.43 \pm 0.58)\%$, $(99.56 \pm 0.48)\%$, and $(99.69 \pm 0.37)\%$ in $\Upsilon(1S)$ decays, $\Upsilon(2S)$ decays, and continuum productions in data, and $\varepsilon_{J/\psi}^{\text{MC}} = 99.9\%$ in the signal MC simulations. We correct the efficiencies by the ratios $\varepsilon_{J/\psi}^{\text{data}}/\varepsilon_{J/\psi}^{\text{MC}}$, and take the errors of the ratios to be the systematic uncertainties, i.e., 0.6% in the $\Upsilon(1S)$ decays, 0.5% in the $\Upsilon(2S)$ decays and 0.4% in the continuum productions. The efficiencies of the requirement $M_{\text{recoil}}^2(pJ/\psi) > 10 \text{ GeV}^2/c^4$ are 98.9%, 99.9%, and 99.9% in signal MC simulations for the $\Upsilon(1S)$ decays, the $\Upsilon(2S)$ decays, and the continuum productions. Since all the MC simulations of the P_c^+ decay model and no- P_c^+ process show efficiencies higher than 98.5%, we take 1.5% as the systematic uncertainty of the requirement on $M_{\text{recoil}}^2(pJ/\psi)$. According to the world average values [29], $\mathcal{B}(J/\psi \rightarrow \ell^+\ell^-)$ ($\ell = e, \mu$) contributes a systematic uncertainty of 0.6%. By varying the photon energy cutoff by 50 MeV in the simulation of ISR, we determine the change of $1 + \delta_{\text{ISR}}$ to be 0.01 and take 1.0% to be the conservative systematic uncertainty in measuring the cross section $\sigma(e^+e^- \rightarrow pJ/\psi + \text{anything})$ at $\sqrt{s} = 10.52$ GeV. There are uncertainties in modeling the final states in the MC simulations. In the hadronization of $q\bar{q}$, we vary the mass and width of X by 200 MeV/ c^2 and 500 MeV, which have differences in efficiency that 2.6% in the $\Upsilon(1S)$ decays, 1.9% in the $\Upsilon(2S)$ decays and 2.3% in the continuum production, respectively. Considering that the proton candidate may come from Λ decay, we simulate the MC samples of $\Upsilon(1, 2S) \rightarrow pJ/\psi + \bar{\Lambda} + (s\bar{q})$ and find the efficiency differences, from those of P_c^+ signal MC samples, of 1.1% in $\Upsilon(1S)$ decays, 1.2% in $\Upsilon(2S)$ decays, and 1.1% in continuum production. We sum the two sources and obtain the system-

atic uncertainties in modeling the final states in MC simulations to be 2.8%, 2.3%, and 2.6% in $\Upsilon(1S)$ decays, $\Upsilon(2S)$ decays, and continuum productions at $\sqrt{s} = 10.52$ GeV. The uncertainties of the total numbers of $\Upsilon(1S)$ events and $\Upsilon(2S)$ events are 2.2% and 2.3% in the Belle data samples [20, 21]. The common uncertainty in the integrated luminosities for the $\Upsilon(1S)$, $\Upsilon(2S)$, and continuum data samples is 1.4%, which is canceled in calculating the scale factor f_{scale} . The statistical uncertainties of the signal MC samples are 0.5% in common. Assuming these uncertainties are independent and sum them in quadrature, we obtain the total systematic uncertainties to be 4.6% in $\mathcal{B}[\Upsilon(1S) \rightarrow pJ/\psi + \text{anything}]$, 4.4% in $\mathcal{B}[\Upsilon(2S) \rightarrow pJ/\psi + \text{anything}]$, and 4.3% in $\sigma(e^+e^- \rightarrow pJ/\psi + \text{anything})$ at $\sqrt{s} = 10.52$ GeV.

In determining the upper limits of P_c^+ productions in $\Upsilon(1, 2S)$ decays, most of the systematic uncertainties are the same as those listed in Table III, with the exception of the modeling of pJ/ψ in signal MC simulations and additional uncertainties in fits. To evaluate these, we do the similar studies, including varying the mass and width of $X \rightarrow q\bar{q}$ and simulating the MC sample of $\Upsilon(1, 2S) \rightarrow P_c^+ + \bar{\Lambda} + (s \bar{q})$. We replace the uncertainties in modeling by 3.3% in $\Upsilon(1S)$ decays and 2.9% in $\Upsilon(2S)$ decays in Table III. Therefore, the total systematic uncertainties of P_c^+ productions in $\Upsilon(1S)$ decays and $\Upsilon(2S)$ decays are 5.0% and 4.7%, respectively. To estimate the systematic uncertainty of $f_{\text{no}P_c}$ in the fits, we investigate the difference in the yield when using an ARGUS function to replace the histogram PDF obtained from the no- P_c^+ MC simulation [32]. We change the masses and the widths of the P_c^+ states by 1σ according to LHCb measurement [15]. As before, we take the highest values of $N_{\text{sig}}^{\text{UL}}(P_c^+)$ to calculate the upper limit of P_c^+ production in the $\Upsilon(1, 2S)$ inclusive decays.

VI. SUMMARY

We study the pJ/ψ final states in $\Upsilon(1, 2S)$ inclusive decays and search for the $P_c(4312)^+$, $P_c(4440)^+$ and $P_c(4457)^+$ signals. To study the production of pJ/ψ in the $\Upsilon(1, 2S)$ data samples, we also investigate the pJ/ψ final state in the Belle continuum data sample. We determine the branching fractions to be $\mathcal{B}[\Upsilon(1S) \rightarrow pJ/\psi + \text{anything}] = (4.27 \pm 0.16 \pm 0.20) \times 10^{-5}$ and $\mathcal{B}[\Upsilon(2S) \rightarrow pJ/\psi + \text{anything}] = (3.59 \pm 0.14 \pm 0.16) \times 10^{-5}$, and the cross section of continuum production to be $\sigma(e^+e^- \rightarrow pJ/\psi + \text{anything}) = (57.5 \pm 2.1 \pm 2.5)$ fb at $\sqrt{s} = 10.52$ GeV. No significant P_c^+ signals exist in the Belle $\Upsilon(1, 2S)$ data samples. We determine the upper limits of P_c^+ productions in $\Upsilon(1, 2S)$ inclusive decays to be

$$\mathcal{B}[\Upsilon(1S) \rightarrow P_c(4312)^+ + \text{anything}] \cdot \mathcal{B}[P_c(4312)^+ \rightarrow pJ/\psi] < 4.5 \times 10^{-6}, \quad (5)$$

$$\mathcal{B}[\Upsilon(1S) \rightarrow P_c(4440)^+ + \text{anything}] \cdot \mathcal{B}[P_c(4440)^+ \rightarrow pJ/\psi] < 6.8 \times 10^{-6}, \quad (6)$$

$$\mathcal{B}[\Upsilon(1S) \rightarrow P_c(4457)^+ + \text{anything}] \cdot \mathcal{B}[P_c(4457)^+ \rightarrow pJ/\psi] < 4.9 \times 10^{-6}, \quad (7)$$

$$\mathcal{B}[\Upsilon(2S) \rightarrow P_c(4312)^+ + \text{anything}] \cdot \mathcal{B}[P_c(4312)^+ \rightarrow pJ/\psi] < 5.3 \times 10^{-6}, \quad (8)$$

$$\mathcal{B}[\Upsilon(2S) \rightarrow P_c(4440)^+ + \text{anything}] \cdot \mathcal{B}[P_c(4440)^+ \rightarrow pJ/\psi] < 7.2 \times 10^{-6}, \quad (9)$$

$$\mathcal{B}[\Upsilon(2S) \rightarrow P_c(4457)^+ + \text{anything}] \cdot \mathcal{B}[P_c(4457)^+ \rightarrow pJ/\psi] < 2.4 \times 10^{-6}, \quad (10)$$

at 90% credibility.

ACKNOWLEDGMENTS

This work, based on data collected using the Belle detector, which was operated until June 2010, was supported by the Ministry of Education, Culture, Sports, Science, and Technology (MEXT) of Japan, the Japan Society for the Promotion of Science (JSPS), and the Tau-Lepton Physics Research Center of Nagoya University; the Australian Research Council including grants DP210101900, DP210102831, DE220100462, LE210100098, LE230100085; Austrian Federal Ministry of Education, Science and Research (FWF) and FWF Austrian Science Fund No. P 31361-N36; National Key R&D Program of China under Contract No. 2022YFA1601903, National Natural Science Foundation of China and research grants No. 11575017, No. 11761141009, No. 11705209, No. 11975076, No. 12135005, No. 12150004, No. 12161141008, and No. 12175041, and Shandong Provincial Natural Science Foundation Project ZR2022JQ02; the Czech Science Foundation Grant No. 22-18469S; Horizon 2020 ERC Advanced Grant No. 884719 and ERC Starting Grant No. 947006 “InterLeptons” (European Union); the Carl Zeiss Foundation, the Deutsche Forschungsgemeinschaft, the Excellence Cluster Universe, and the VolkswagenStiftung; the Department of Atomic Energy (Project Identification No. RTI 4002), the Department of Science and Technology of India, and the UPES (India) SEED finding programs Nos. UPES/R&D-SEED-INFRA/17052023/01 and UPES/R&D-SOE/20062022/06; the Istituto Nazionale di Fisica Nucleare of Italy; National Research Foundation (NRF) of Korea Grant Nos. 2016R1D1A1B-02012900, 2018R1A2B3003643, 2018R1A6A1A06024970, RS202200197659, 2019R1I1A3A-01058933, 2021R1A6A1A03043957, 2021R1F1A1060423, 2021R1F1A1064008, 2022R1A2C-1003993; Radiation Science Research Institute, Foreign Large-size Research Facility Application Supporting project, the Global Science Experimental Data Hub Center of the Korea Institute of Science and Technology Information and KREONET/GLORIAD; the Polish Ministry of Science and Higher Education and the National Science Center; the Ministry of Science and Higher Education of the Russian Federation and the HSE University Basic Research Program, Moscow; University of Tabuk research grants S-1440-0321, S-0256-1438, and S-0280-1439 (Saudi Arabia); the Slovenian Research Agency Grant Nos. J1-9124 and P1-0135; Ikerbasque, Basque Foundation for Science, and the State Agency for Research of the Spanish Ministry of Science and Innovation through Grant No. PID2022-136510NB-C33 (Spain); the Swiss National Science Foundation; the Ministry of Education and the National Science and Technology Council of Taiwan; and the United States Department of Energy and the National Science Foundation. These acknowledgements are not to be interpreted as an endorsement of any statement made by any of our institutes, funding agencies, governments, or their representatives. We thank the KEKB group for the excellent operation of the accelerator; the KEK cryogenics group for the efficient operation of the solenoid; and the KEK computer group and the Pacific Northwest National Laboratory (PNNL) Environmental Molecular Sciences Laboratory (EMSL) computing group for strong computing support; and the National Institute of Informatics, and Science Information NETwork 6 (SINET6) for valuable network support.

-
- [1] M. Gell-Mann, *Phys. Lett.* **8**, 214 (1964).
 - [2] N. Brambilla *et al.*, *Eur. Phys. J. C* **71**, 1534 (2011).
 - [3] S. L. Olsen, T. Skwarnicki and D. Zieminska, *Rev. Mod. Phys.* **90**, 015003 (2018).

- [4] S. K. Choi *et al.* (Belle Collaboration), Phys. Rev. Lett. **91**, 262001 (2003).
- [5] S. K. Choi *et al.* (Belle Collaboration), Phys. Rev. Lett. **100**, 142001 (2008).
- [6] R. Aaij *et al.* (LHCb Collaboration), Phys. Rev. Lett. **112**, 222002 (2014).
- [7] R. Mizuk *et al.* (Belle Collaboration), Phys. Rev. D **78**, 072004 (2008).
- [8] A. Bondar *et al.* (Belle Collaboration), Phys. Rev. Lett. **108**, 122001 (2012).
- [9] M. Ablikim *et al.* (BESIII Collaboration), Phys. Rev. Lett. **110**, 252001 (2013).
- [10] Z. Q. Liu *et al.* (Belle Collaboration), Phys. Rev. Lett. **110**, 252002 (2013).
- [11] M. Ablikim *et al.* (BESIII Collaboration), Phys. Rev. Lett. **111**, 242001 (2013).
- [12] X. L. Wang *et al.* (Belle Collaboration), Phys. Rev. D **91**, 112007 (2015).
- [13] M. Ablikim *et al.* (BESIII Collaboration), Phys. Rev. D **96**, 032004 (2017).
- [14] R. Aaij *et al.* (LHCb Collaboration), Phys. Rev. Lett. **115**, 072001 (2015).
- [15] R. Aaij *et al.* (LHCb Collaboration), Phys. Rev. Lett. **122**, 222001 (2019).
- [16] C. E. Carlson, J. R. Hiller and R. J. Holt, Annu. Rev. Nucl. Part. Sci. **47**, 395 (1997).
- [17] D. M. Asner *et al.* (CLEO Collaboration), Phys. Rev. D **75**, 012009 (2007).
- [18] H. Albrecht *et al.* (ARGUS Collaboration), Phys. Lett. B **236**, 102 (1990).
- [19] J. P. Lees *et al.* (BABAR Collaboration), Phys. Rev. D **89**, 111102(R) (2014).
- [20] C. P. Shen *et al.* (Belle Collaboration), Phys. Rev. D **82**, 051504 (2010).
- [21] X. L. Wang *et al.* (Belle Collaboration), Phys. Rev. D **84**, 071107 (2011).
- [22] A. Abashian *et al.* (Belle Collaboration), Nucl. Instrum. Methods A **479**, 117 (2002); also see detector section in J. Brodzicka *et al.*, Prog. Theor. Exp. Phys. **2012**, 04D001 (2012).
- [23] D. J. Lange, Nucl. Instrum. Methods A **462**, 152 (2001).
- [24] T. Sjostrand, S. Mrenna, and P. Skands, J. High Energy Phys. **05**, 026 (2006).
- [25] R. Brun *et al.*, GEANT 3.21, CERN DD/EE/84-1, 1984.
- [26] E. Nakano, Nucl. Instrum. Methods A **494**, 402 (2002).
- [27] K. Hanagaki *et al.*, Nucl. Instrum. Methods A **485**, 490 (2002).
- [28] A. Abashian *et al.*, Nucl. Instrum. Methods A **491**, 69 (2002).
- [29] R. L. Workman *et al.* (Particle Data Group), Prog. Theor. Exp. Phys. 2022083C012022 and 2023 update.
- [30] S. Actis *et al.*, Eur. Phys. J. C **66**, 585 (2010).
- [31] X. K. Dong, X. H. Mo, P. Wang, and C. Z. Yuan, Chin. Phys. C **44**, 083001 (2020).
- [32] H. Albrecht *et al.* (ARGUS Collaboration), Phys. Lett. B **241**, 278 (1990).